HHS Public Access

Author manuscript

Biomaterials. Author manuscript; available in PMC 2026 February 01.

Published in final edited form as:

Biomaterials. 2025 February ; 313: 122767. doi:10.1016/j.biomaterials.2024.122767.

Intravascular delivery of an MK2 inhibitory peptide to prevent restenosis after angioplasty

J. William Tierney[a], **R. Paolo Francisco**[a], **Fang Yu**[a], **Jinqi Ma**[a], **Joyce Cheung-Flynn**[b], **Megan C. Keech**[a], **Richard D'Arcy**[a,c], **Veeraj M. Shah**[a], **Anna R. Kittel**[a], **Devin J. Chang**[a], **Joshua T. McCune**[a], **Mariah G. Bezold**[a], **Adrian N. Aligwekwe**[d,e], **Rebecca S. Cook**[a,f], **Joshua A. Beckman**[g], **Colleen M. Brophy**[b,h], **Craig L. Duvall**[a,*]

[a]Department of Biomedical Engineering, Vanderbilt University, Nashville, TN, 37235, USA

[b]Division of Vascular Surgery, Department of Surgery, Vanderbilt University Medical Center, Nashville, TN, 37232, USA

[c]Chemical Engineering, School of Engineering of Matter, Transport and Energy, Arizona State University, Tempe, AZ, USA

[d]Medical Scientist Training Program, Vanderbilt University School of Medicine, Nashville, TN, 37232, USA

[e]North Carolina State University, Raleigh, NC, 27695, USA

[f]Vanderbilt-Ingram Cancer Center, Vanderbilt University Medical Center, Nashville, TN, 37232, USA

[g]Department of Internal Medicine, University of Texas Southwestern Medical Center, Dallas, TX, 75390, USA

[h]Veterans Affairs Medical Center, VA Tennessee Valley Healthcare System, Nashville, TN, 37212, USA

Abstract

[*]Corresponding author. 5824 Stevenson Center, Nashville, TN, 37232, USA. craig.duvall@vanderbilt.edu (C.L. Duvall).

CRediT authorship contribution statement

J. William Tierney: Writing – original draft, Validation, Project administration, Methodology, Investigation, Formal analysis, Conceptualization. **R. Paolo Francisco:** Writing – review & editing, Investigation. **Fang Yu:** Methodology, Investigation. **Jinqi Ma:** Investigation. **Joyce Cheung-Flynn:** Writing – review & editing, Validation, Methodology, Conceptualization. **Megan C. Keech:** Investigation. **Richard D'Arcy:** Resources. **Veeraj M. Shah:** Investigation. **Anna R. Kittel:** Investigation. **Devin J. Chang:** Methodology, Investigation. **Joshua T. McCune:** Methodology. **Mariah G. Bezold:** Methodology. **Adrian N. Aligwekwe:** Investigation. **Rebecca S. Cook:** Visualization. **Joshua A. Beckman:** Writing – review & editing, Conceptualization. **Colleen M. Brophy:** Writing – review & editing, Supervision, Conceptualization. **Craig L. Duvall:** Writing – review & editing, Supervision, Project administration, Funding acquisition, Conceptualization.

Declaration of competing interest

The authors declare that they have no known competing financial interests or personal relationships that could have appeared to influence the work reported in this paper.

Appendix A. Supplementary data

Supplementary data to this article can be found online at https://doi.org/10.1016/j.biomaterials.2024.122767.

Peripheral artery disease is commonly treated with balloon angioplasty, a procedure involving minimally invasive, transluminal insertion of a catheter to the site of stenosis, where a balloon is inflated to open the blockage, restoring blood flow. However, peripheral angioplasty has a high rate of restenosis, limiting long-term patency. Therefore, angioplasty is sometimes paired with delivery of cytotoxic drugs like paclitaxel to reduce neointimal tissue formation. We pursue intravascular drug delivery strategies that target the underlying cause of restenosis - intimal hyperplasia resulting from stress-induced vascular smooth muscle cell switching from the healthy contractile into a pathological synthetic phenotype. We have established MAPKAP kinase 2 (MK2) as a driver of this phenotype switch and seek to establish convective and contact transfer (coated balloon) methods for MK2 inhibitory peptide delivery to sites of angioplasty. Using a flow loop bioreactor, we showed MK2 inhibition in *ex vivo* arteries suppresses smooth muscle cell phenotype switching while preserving vessel contractility. A rat carotid artery balloon injury model demonstrated inhibition of intimal hyperplasia following MK2i coated balloon treatment *in vivo*. These studies establish both convective and drug coated balloon strategies as promising approaches for intravascular delivery of MK2 inhibitory formulations to improve efficacy of balloon angioplasty.

Keywords

Peripheral artery disease; Restenosis; Drug delivery; Intravascular delivery; Drug coated balloons

1. Introduction

Catheter-based, transluminal angioplasty can restore blood flow at sites of arterial narrowing, but the balloon-related injury to the arterial wall commonly leads to restenosis, or re-occlusion, of the artery [1]. In coronary artery interventions, balloon angioplasty is routinely paired with stenting to maintain vessel patency. In other vascular beds, such as the lower extremities, stenting is less practical; for example, the risk of stent fracture and failure is increased as a result of adverse flow and radial stress conditions [2–4]. Without stenting, angioplasty treatment alone has a 60 % restenosis rate at 12 months [5]. Therefore, there is an unmet need to develop a novel, non-stent therapy to be paired with angioplasty to prevent vessel restenosis in peripheral arteries.

Multiple factors lead to restenosis, with the most prominent cause being intimal hyperplasia (IH) driven by smooth muscle cell (SMC) contractile-to-synthetic phenotype switching [6,7]. Mechanical damage and inflammatory signaling due to vessel distention induces healthy contractile SMCs to transition to a more proliferative, inflammatory, and fibrotic synthetic state [8]. Synthetic SMC proliferation and extracellular matrix (ECM) deposition creates a neointima that occludes the arterial lumen. Cytotoxic and cytostatic drugs like paclitaxel and sirolimus, respectively, have been integrated into drug coated balloons (DCBs) to combat SMC over-proliferation to reduce restenosis [9]. These drugs non-selectively block proliferating cells, including endothelial cells, thus increasing the risk of thrombosis [10]. Additionally, paclitaxel DCBs are currently the only approved DCB for use in lower extremity arteries, and they do not show significant improvement in limb salvage, survival, or restenosis in a recent meta-analysis [11]. Consequently, there is a need for new

therapeutic strategies to be paired with angioplasty that target the molecular underpinnings of IH.

Our recent studies have established MAPKAP kinase 2 (MK2) as a driver of SMC phenotype switching and a promising target for preventing IH development [12,13]. Formulation of an MK2 inhibitory peptide (MK2i) with a pH-responsive polymer (PPAA) electrostatically forms MK2i nanopolyplexes (MK2i-NPs) that are ~120 nm in diameter and can be made in the presence of lactosucrose to yield a stable, lyophilized preparation [13,14]. Relative to free MK2i peptide, MK2i-NPs increase cellular uptake and promote endosome escape, which promotes higher cytoplasmic bioavailability and duration of action [15–17]. Topical delivery of MK2i-NPs to explanted venous tissue blocks IH in several *ex vivo* and *in vivo* models of bypass grafting [12,13]. Instead of blocking or killing proliferating cells, MK2i-NPs alter the gene expression landscape to preserve the healthy contractile SMC phenotype while reducing inflammation, proliferation, and ECM production. However, non-invasive, transluminal angioplasty procedures do not allow for topical treatment of explanted tissues. As the majority of all lower extremity revascularization procedures are catheter-based [18], it is salient to create methods that enable intravascular delivery of MK2i + PPAA formulations into the arterial wall *in vivo* in conjunction with angioplasty procedures.

Here, we seek to develop and validate convective delivery and layer-by-layer (LbL) drug coated balloons for intravascular application of MK2i + PPAA formulations for the prevention of angioplasty-induced SMC phenotype switching and restenosis. Convective delivery of drugs to the vascular wall has been achieved by porous balloons that inject therapy through small openings in an inflated balloon [19,20]. *Ex vivo* pressure-mediated transfection was used in a clinical trial to test delivery of an E2F decoy to vein graft explants for IH prevention post-transplant [21]. Here, we model the use of a specialized occlusion perfusion catheter that uses two occlusion balloons to isolate a targeted segment of an artery to be treated. The occluded lumen space is filled with a solution of the drug and pressurized to force the drug into the vascular wall. The occlusion perfusion catheter has shown promise in clinical trials for paclitaxel delivery, achieving FDA approval [22,23], and it has been tested preclinically to administer paclitaxel [24] and aptamers [25] to *ex vivo* arteries. For comparison, we also pursue a layer-by-layer (LbL) coating of MK2i + PPAA onto angioplasty balloons for contact transfer to the tissue at the site of balloon deployment. LbL coatings of angioplasty balloons have been used previously to deliver biologic drug cargo such as polymeric nanoparticles [26] with some success. The opposite charges of (+)MK2i and (−)PPAA make them suitable candidates for electrostatic LbL balloon coating. We sought to test whether these delivery strategies enable bioactive delivery of MK2i + PPAA formulations and if these treatments preserve vessel contractility and prevent SMC phenotype switching and IH after angioplasty.

2. Methods

Materials:

Angioplasty balloons (Boston Scientific) were purchased from Medical Materials, Inc. MK2i peptide (YARAAARQAR-AKALARQLGVAA) was synthesized by EzBioLab

(Carmel, IN) at a scale of 500 mg with a purity ≥95 % as determined by mass spectrometry. Antibodies against P-CREB (87G3), CREB (86B10), MYH (D8H8), and vimentin (VIM) (D21H3) were purchased from Cell Signaling Technologies. Antibodies against PCNA (ab29), SM22 (ab14106), CD3 (ab16669), and CD68 (ab125212) were purchased from Abcam. Anti-Fibronectin (FN) antibody was purchased from Millipore Sigma (F6140).

PPAA Synthesis:

The PPAA polymer was prepared utilizing bulk RAFT polymerization, adapting protocols outlined in the literature [12, 27]. The monomer 2-propylacrylic acid (2-PAA) was produced following the approach outlined by Ferritto et al. [28]. The 4-cyano-4-(ethylsulfanylthiocarbonyl) sulfanylpentanoic acid chain transfer agent (CTA) was synthesized as in previous works [29]. In the polymerization setup, a precise mixture of 2-PAA monomer, 2,2′-azo-bis-isobutyrylnitrile (AIBN, purified via recrystallization from a methanolic solution) as the initiation agent, and the CTA were combined, maintaining a molar ratio of CTA:AIBN:monomer at 1:1:219; this ratio was calculated to target a final polymer molecular weight of approximately 25,000 g/mol upon complete monomer conversion. The mixture was added to a Schlenk tube equipped with a magnetic stirrer and exposed to three cycles of freezing, vacuum application, and thawing. It was then flushed with nitrogen gas for 30 min and kept under nitrogen throughout the polymerization. The reaction was initiated upon heating the mixture to 70 °C. The progress of the polymerization was monitored over 72 h by observing the viscosity and evaluating monomer conversion. The synthesized polymer was exposed to air, diluted into dimethylformamide (DMF), precipitated into cold ethyl acetate (x3) and diethyl ether (x2), and dried under vacuum overnight. The resulting polymer was dissolved into neutralized phosphate buffer (10 mM) and was then dialyzed in a 12–14 kDa MWCO membrane for 2 days, at which point the dialysis was changed to 0.01 mM phosphate buffer for an additional day. The product was freeze dried and then characterized by gel permeation chromatography (GPC) using an Agilent 1200 series GPC system equipped with a mini-DAWN T-rex light scattering detector, a variable wavelength detector, and a refractive index detector. The system was configured with three TSKGel Alpha columns (Tosoh) in series and operated at 60 °C. The eluent used was HPLC grade DMF with 0.1 % LiBr, flowing at a rate of 1 mL/min. Data analysis was conducted using Astra V software (Wyatt Technology), with calibration performed using PMMA and PEG standards supplied by Agilent. Additional verification of the polymer's purity, composition, and molecular weights was carried out through ^{1}H NMR analysis.

Fluorescent MK2i conjugation:

Fluorescent MK2i was made using an Alexa Fluor NHS Ester kit (Thermo Fisher). 50 μL of the dye solution was added to 1 mL of 10 mg/mL MK2i in 0.1 M sodium bicarbonate buffer. The dye-MK2i solution was put on a shaker at RT for 1 h. The conjugated peptide was then separated and dissolved in PBS using a PD-10 column. Conjugation and fluorescent peptide concentration was quantified by measuring absorbance at 260 and 280 and using the proper correction factor for the Alexa Fluor dye. Alexa 488 (Ex/Em 490nm/525 nm) was used for flow cytometry studies and Alexa 568 (Ex/Em 578nm/603 nm) was used for all other studies.

MK2i-NP Formulation:

To prepare lyophilized MK2i-NPs for long-term storage, a previously described method was used [14]. Briefly, MK2i-NPs were formulated at concentrations of 500 μM MK2i and 50 μM PPAA to form a 10X stock with 300 mM lactosucrose added as a lyoprotectant to the NP solution. The NPs were then syringe-filtered through a 0.45 μm pore size polytetrafluoroethylene (PTFE) filter and separated into 100 μL aliquots. They were then frozen to −80 °C for 24 h and lyophilized. NPs were reconstituted for 30 min before use by addition of 100 μL of sterile water before being diluted in pH 8 PBS to achieve the desired concentration for dosing.

Layer-by-layer balloon coating:

Angioplasty balloons were obtained from Medical Materials, Inc. To establish a positively charged surface, the balloon was air plasma treated with a Harrick benchtop plasma cleaner for 2 min to oxidize the surface and then immediately placed into a 1 w/w% solution of (3-Aminopropyl)triethoxysilane (APTES) in 50 % ethanol for 3 h. To coat the balloon, solutions of MK2i and PPAA were made in methanol at the concentrations indicated. The balloon was then dipped for 3–5 s in the PPAA solution and allowed to air dry for 1 min before a second dip and dry to establish a thorough coating of PPAA on the balloon. This process was then repeated with the MK2i solution to create a layer on top of the PPAA layer. These steps were repeated to create 6 PPAA/MK2i bilayers on the balloon. Balloon layering was confirmed by using Alexa-568 labeled MK2i (MK2i-568) and visualizing the coating on IVIS and SEM. In some cases, the excipient lactosucrose (50 mg/mL) was included in the PPAA coating solution as indicated.

Balloon loading and release quantification:

Angioplasty balloons (2.5 mm × 20 mm, Maverick OTW, Boston Scientific) were coated with PPAA and MK2i-568 and then soaked in PBS with calcium and magnesium for 3 min to measure balloon release. The balloons were then soaked again in DMSO under sonication for 3 min to remove any remaining surface-associated MK2i. The fluorescence of the PBS and DMSO solutions was measured on a TECAN Infinite M1000 Pro plate reader and compared to a standard curve of MK2i-568 in PBS and DMSO, respectively.

Rat aorta harvest:

Retired breeder Sprague-Dawley rats (Charles River Laboratories) were euthanized with CO_2. The chest cavity was opened, and the fascia and connective tissue surrounding the thoracic aorta were carefully removed. Branches from the aortas were cauterized with a Bovie cautery pen (Medline) to allow for vessel pressurization. The harvested aortas were stored in DMEM (+25 mM HEPES, +4.5 g/L D-glucose, +4 mM L-glutamine, +3 % FBS, +1 % Antibiotic/Antimycotic) at 37 °C until experimentation.

Aorta treatment:

Harvested aortas were damaged with an angioplasty balloon prior to treatment (3x, 15 s each, 25 % overstretch). Coated balloons were then inserted into the aorta and pressurized for 3 min in DMEM (+25 mM HEPES, +4.5 g/L D-glucose, +4 mM L-glutamine, +3 %

FBS, +1 % Antibiotic/Antimycotic), with deflation and reinflation at each minute mark to allow for maximum release and tissue transfer. After 3 min, the balloon was deflated and removed. The treated artery was then washed briefly with DMEM and then processed for further experimentation or data collection.

Angioplasty damage was induced the same for tests with convective delivery. After the balloon was removed, the aortas were connected to a pressure sensor and filled with treatment solution (50 μM MK2i, 50 μM preformed MK2i-NPs, or 5 μM PPAA sequentially followed by solution of 50 μM MK2i (PPAA→MK2i)). The open end of the aorta was then clamped, and a syringe was used to pressurize the treatment solution within the artery to 150 mmHg. This pressure was held for 3 min (for PPAA- > MK2i, each step was held for 3 min). The treated aorta was then disconnected from the clamp and pressure sensor, washed briefly to remove any excess MK2i, and then processed for further experimentation or data collection.

Delivery visualization and quantification:

Immediately after treatment, a 3–5 mm segment from the center of the aorta was placed into OCT and frozen for cryosectioning. Samples were cut into 10 μm sections and secured onto slides using ProLong Gold Antifade mounting media with DAPI. After drying, the slides were scanned on a Nikon Eclipse Ti confocal microscope to measure the intensity of the fluorescent MK2i within the arterial cross-section. An ROI was drawn around the outside and inside edges of the vessel using automatic ROI detection on the DAPI channel. Then, total intensity of fluorescent MK2i within the arterial wall was calculated by subtracting the intensity of the inner (lumen) region from the intensity of the total region. Similar ROI approaches were used to calculate the area of the arterial wall. For data presentation, the fluorescence intensity was normalized to the area for each sample. Additionally, a spatial delivery profile as a function of depth into the arterial wall was created by drawing a line (lumen to adventitia) at 8 evenly spaced points around the arterial wall and averaging the fluorescence intensity along those lines.

Flow Cytometry:

After convective or coated balloon aorta treatment with MK2i-568 formulations, vessel samples were incubated in DMEM (+25 mM HEPES, +4.5 g/L D-glucose, +4 mM L-glutamine, +3 % FBS, +1 % Antibiotic/Antimycotic) for 1 h at 37 °C to allow time for cell uptake. The aortas were subsequently transferred to 500 μL of cold PBS +1 % FBS and cut with scissors into small (~1 mm square) pieces. Digestion media in DMEM was then added to the PBS/tissue tube (500 μL) to achieve a final enzyme concentration of 0.7 mg/mL liberase, 4 mg/mL collagenase, and 0.2 mg/mL DNase, and the tubes were placed in a 37 °C incubator on a shaker for ~90 min or until digestion was apparent. After incubation, the samples were filtered through a 70 μm cell strainer and centrifuged at 500 g for 8 min. The resulting cell pellet was resuspended in 200 μL of FACS buffer (PBS +/+, 1 % FBS, 2 mM EDTA) and transferred to a 96 well plate for flow cytometry. Cells were read for fluorescence on a Guava easyCyte HT, and the resulting data was processed in FlowJo.

Flow Loop Bioreactor Setup:

To prepare the bioreactor system for aorta culture under flow, a sterile 4 mm biopsy punch was used to make holes in sterile 50 mL conical tubes. Connecting tubes were sterilized with ethanol and washed through with 3 % hydrogen peroxide followed by DI water. Treated aortas were hung inside each 50 mL tube and stretched to 130 % of their length *ex vivo* to simulate physiological tension. The media used was based on methods previously described by Wang et al. [30] and was created by mixing 50 % DMEM (+25 mM HEPES, +4.5 g/L D-glucose, +4 mM L-glutamine) and 50 % VascuLife growth media (VWR) supplemented with 1 % Antibiotic/Antimycotic and 30 g/L dextran to increase the viscosity of the media to be similar to blood. Flow loop media was further supplemented to 20 % FBS to promote VSMC phenotype switching within the arteries. Aortas were connected to tubing with plastic cannulas and secured with sterile sutures. The flow rate was set to 6 mL/min to create 4–5 dyn/cm^2 shear stress, which is similar to that of atherosclerotic arterial regions [31]. As in Wang et al. [30], Doriot's equation was used to calculate the ideal flow rate with a set viscosity of 0.043 dyn s/cm^2 based on an average arterial diameter of 1.8 mm, determined from histological sections. The media flowing through the aortas was replaced every other day (50 mL reservoir), while 1/3 of the media circulating around the aorta was replenished every day (50 mL of 150 mL total).

MTT Viability:

Upon conclusion of flow bioreactor culture, a small ring was dissected from each aorta and was further incubated in 400 μL PBS with 2.5 mg/mL (3-(4,5-dimethylthiazol-2-yl)-2,5-diphenyltetrazolium bromide (MTT) for 30 min. After incubation, the rings were transferred to 400 μL of Cellosolve to dissolve the formazan crystals for 1 h on a rocker at RT. Then, 100 μL of the Cellosolve solution was transferred to a 96 well plate for each sample. The absorbance at 590 nm was read on a TECAN Infinite M1000 Pro plate reader and normalized to the mass of the aortic ring. Relative viability was determined by comparing samples that had been maintained in the flow bioreactor to freshly harvested rat aorta samples.

Western Blotting for P-CREB inhibition:

Acute (1hr) inhibition of cAMP-response element binding protein (CREB) phosphorylation was assessed in rat aorta samples divided in half. One half underwent initial balloon damage, followed by administration of vehicle control (PBS for convective delivery, uncoated balloon for balloon delivery) for 3 min. The other half of each sample underwent a convective or DCB MK2i treatment. The samples were incubated for 1hr after balloon damage/treatment in DMEM (+25 mM HEPES, +4.5 g/L D-glucose, +4 mM L-glutamine, +3 % FBS, +1 % Antibiotic/Antimycotic) before being processed for western blotting. For extended CREB inhibition, aorta samples were incubated in the flow loop for 24 h, 3 days, or 7 days after treatment. Each aorta was then divided in half and transferred to flow loop media with or without 60 μM LPA (or 240 μM LPA for 7 day samples) for 2 h. The samples were then flash frozen in liquid nitrogen. Frozen aortas were homogenized with a tissue pulverizer and lysed in RIPA buffer with protease and phosphatase inhibitors (Roche). The tissue homogenates were vortexed for 15 min at 4C and then centrifuged at 12,000g for 15 min

at 4C to collect the supernatant. Protein concentration was quantified using a BCA Assay kit (Pierce). Protein (40 μg) was resolved on 4–20 % SDS-PAGE gels and transferred to a nitrocellulose membrane using the Invitrogen iBlot 2. Blots were incubated in primary P-CREB antibody (1:1000) overnight at 4C and were then incubated in the secondary antibody (Li-Cor 926–32211, 926–32210, 1:5000 dilution) for 1hr at room temperature. Blots were imaged on a LiCor Odyssey Fc. The blots were then stripped and stained for CREB using the same method.

MK2i Delivery and Retention Quantification:

Treated aorta samples were incubated in the flow loop bioreactor and then digested in the same digestion medium used for flow cytometry. Aortas were digested in 20x the volume of digestion media relative to their mass. Once the tissue was sufficiently digested, the fluorescence (Ex 578, Em 603) was measured on a TECAN Infinite M1000 Pro plate reader and compared to a standard curve created by doping in known quantities of fluorescent MK2i to digested untreated aorta samples.

Muscle Baths:

Vessel contractility was assessed using a previously established method [32]. In brief, aortic rings were cut (~2 mm thick) and suspended in a muscle bath (Radnoti) containing bicarbonate buffer (120 mM NaCl, 4.7 mM KCl, 1.0 mM MgSO4, 1.0 mM NaH2PO4, 10 mM glucose, 1.5 mM CaCl2, and 25 mM Na2HCO3, pH 7.4) equilibrated with 5 % CO2 at 37 °C. The tissue was maintained at a resting tension of 1 g, manually stretched to three times the resting tension, and maintained at resting tension for an additional 1 h. This produced the maximal force tension relationship. Next, the rings were primed with 110 mM of potassium chloride (with equimolar replacement of sodium chloride in bicarbonate buffer) to determine functional viability. Rings were then stimulated with escalating doses of phenylephrine (PE) to determine contractile responses to agonist. Force measurements were obtained using the Radnoti force transducer (model 159901A, Radnoti) interfaced with a PowerLab data acquisition system and LabChart software (AD Instruments Inc, Colorado Springs, CO). Contractile responses were defined by stress, calculated using force generated by tissues as follows: stress ($\times 10^5$ N/m^2) = force (g) × 0.0987/area, where area = wet weight (mg)/at maximal length (mm)]/1.055.

Fluorescence Immunohistochemistry:

Rat aortas were balloon damaged and either treated or left untreated before incubation in the flow loop bioreactor for 7 days. Aorta samples were then fixed with 10 % neutral buffered formalin and embedded in paraffin. Samples were cut into 5 μm sections and allowed to dry on slides overnight. The slides were then baked in a 60 °C oven for 1 h, rehydrated with xylene, 100 % EtOH, and 95 % EtOH washes, and antigen retrieval was performed in pH 6 citrate buffer at 97 °C for 20 min in an Epredia PT Module. For immunofluorescence, slides were treated with serum-free protein block (Daco) for 20 min followed by fluorescent blocking buffer (Thermo) for 30 min. The slides were then incubated in the primary antibody for 1 h followed by the secondary antibody for another hour, and coverslips were secured onto each slide using ProLong Gold Antifade mounting media with DAPI. Slides were scanned using a Nikon Eclipse Ti confocal microscope. MYH, VIM, PCNA, SM22,

CD68, FN, and P-CREB antibodies were used at a 1:1000 dilution, CD3 antibody was used at 1:500. Secondary antibodies (Invitrogen) were used at a 1:1000 dilution.

Rat carotid artery balloon injury model:

Carotid artery balloon injury was performed as previously described [33]. Briefly, male Sprague Dawley rats (400–550g) were anesthetized with 3 % isoflurane, and the area from the chin to the top of the sternum was shaved. The surgical site was cleaned with iodine, and then an incision was made in a straight line from the chin to the sternum. Glandular tissue, fascia, and muscle was blunt dissected away and retracted to expose the left carotid artery. The proximal common carotid artery was temporarily clamped to cut off blood flow, and the distal external carotid was tied to prevent backflow. Then, on the external carotid artery branch, a small arteriotomy incision was made about 1/4–1/3 of the circumference of the vessel. Through this incision, the deflated angioplasty balloon (1.5 mm×12mm, Emerge OTW, Boston Scientific) was inserted up to the arterial clamp. Then, the clamp was released, and the balloon was inserted further down to the aortic arch. Once the balloon was in place, it was fully inflated with a sterile saline syringe and gently withdrawn with rotation to damage the vessel. When the balloon was close to the arteriotomy incision, it was deflated and inserted again. The inflation and removal were repeated 2 more times to thoroughly damage the artery. Prior to full removal of the balloon, a suture was loosely tied around the external carotid artery proximal to the arteriotomy incision. After 3 rounds of balloon insertion and damage, the balloon was deflated and removed, and the suture around the external carotid artery was quickly tied tight to prevent bleeding from the incision. In animals that were in the treatment group, the carotid artery was instead clamped again prior to balloon removal. A MK2i + PPAA coated balloon (1.5 mm × 12 mm, Emerge OTW, Boston Scientific) was then introduced into the arteriotomy incision and inserted down to the area of balloon damage. This balloon was then inflated at the damaged site for 3 min, with deflation and re-inflation at each minute mark to aid in drug transfer. After treatment, the balloon was deflated and removed, and the external carotid was tied to prevent bleeding. Any other sutures and ligations were then removed, and branching arteries were checked to ensure blood flow. Two weeks after surgery, the rats were euthanized, and the carotid arteries were removed and fixed in 10 % neutral buffered formalin for histology and immunofluorescence staining.

Statistics:

Statistical significance for experiments with more than 2 groups was determined using one-way ANOVA tests with Tukey’s post hoc test. Experiments with 2 groups used Welch’s *t*-test unless otherwise noted. For the study on optimization of balloon loading, statistical significance was determined using a two-way ANOVA with comparisons between groups. For P-CREB Western blot pairwise comparisons at the 1 h time point, significance was determined with ratio paired t tests. Significance for the muscle bath contractility test was determined with a one-way ANOVA and Tukey’s post hoc test on IC50 values determined from linear regression models of the PE vs contraction curves. Analyses were performed in GraphPad Prism 10 software. Results are presented as arithmetic mean ± SD with P values as indicated in the figures or figure legends. P values of less than 0.05 were considered to be significant.

Study approval:

All animal studies were approved by the Vanderbilt University IACUC and conformed to the Guide for the Care and Use of Laboratory Animals (National Academies Press, 2011).

3. Results

Convective delivery and cell uptake of MK2i + PPAA is formulation dependent.

Convective delivery involves isolating the desired segment of the artery after angioplasty, filling in the lumen with a solution of the drug, and pressurizing that solution to drive it into the vascular wall. We tested two different approaches for delivery of a combination of MK2i peptide and the endosomolytic, anionic polymer PPAA (generally referred to as MK2i + PPAA) in *ex vivo* rat aortas (Fig. 1A). In these studies, the aortas were isolated and underwent plain balloon angioplasty (3x, 15 s, 25 % overstretch) before they were filled with the treatment solution and pressurized to 150 mmHg for 3 min. MK2i + PPAA has been shown to be effective in vitro as both pre-formed MK2i-NPs and in sequential delivery of PPAA followed by MK2i (PPAA→MK2i) [27,34]. Therefore, we compared convective delivery of free MK2i to both of these approaches.

Convective delivery of fluorescent MK2i into the vessel wall was apparent for free MK2i and both PPAA + MK2i formulations (MK2i-NPs and PPAA→MK2i), as seen within images of vessel cross-sections (Fig. 1B). Free MK2i had the greatest level of tissue delivery, while MK2i-NPs had a more modest level of delivery, and PPAA→MK2i achieved an intermediate level of delivery (Fig. 1C). Measuring delivery as a function of depth into the vessel wall showed that MK2i is relatively homogeneously distributed throughout the vessel wall for free MK2 and both of the MK2i + PPAA formulations (Fig. 1D). Beyond tissue level analysis, it is critical to assess intracellular delivery of the MK2i peptide which acts on signaling pathways localized to the cellular cytoplasm. Vascular smooth muscle cells were isolated from the treated aortas after 1 h static incubation and ran on a flow cytometer to measure individual cell fluorescence as an indicator or relative uptake of fluorescent MK2i. Despite having less tissue penetration than the other formulations, MK2i-NPs yielded significantly more cellular internalization of MK2i than either MK2i alone or sequential PPAA + MK2i delivery (Fig. 1E).

Layer-by-layer MK2i + PPAA coating of angioplasty balloons to maximize MK2i loading and release.

Next, MK2i + PPAA LbL drug coated balloon methods were optimized for testing in *ex vivo* rat aortas (Fig. 2A). To create a coating of MK2i + PPAA on the surface of a plain angioplasty balloon, a LbL method was implemented (Fig. 2B). The balloon was first surface functionalized with APTES to create a positively charged base layer. Then, the balloon was dip coated using alternating solutions of PPAA and MK2i to create layers of positive and negative charges. Lactosucrose (LS) was tested as an excipient within the PPAA layers to potentially help with tissue transfer and dispersion of the coating upon deployment in tissue. Using fluorescently labeled MK2i, peptide loading onto the surface was confirmed using IVIS (Fig. 2C), and the coating was visualized with SEM (Fig. S1).

Loading and release of MK2i from the surface of the balloons were quantified (Fig. 2D). Initial coating with 6 layers using solutions of 50 μM MK2i and 5 μM PPAA (6 L-50M – 5P) yielded 1.5–2 μg/cm^2 of MK2i loading. Increasing the number of layers (12 L-50M – 5P) and increasing the concentration of the loading solutions (6 L-100M – 10P) both increased the peptide loading, with 6 L-100M – 10P balloons showing the highest MK2i loading of 4.5–5 μg/cm^2. Importantly, each of the LbL protocols was reproducible and showed low variance between samples. When balloons were tested for release in PBS, 12 L-50M – 5P balloons did not show as efficient release of the MK2i from the balloon surface, potentially due to the increased interactions between layers. The higher loading and release of the 6 L-100M – 10P method led us to coat balloons with this strategy for the remaining studies. All DCBs referred to hereforth use the 6 L-100M – 10P method and will be referred to based on whether or not the LS excipient was included (+LS) or not (−LS) during the polymer coating steps.

Although addition of LS to the PPAA layers did not yield any differences in loading and release in PBS, a greater effect of LS inclusion was observed when these balloons were used to treat rat aortas *ex vivo* (Fig. 2E and F). Adding LS increased MK2i transfer to the tissue and had a modest effect on increasing the depth of delivery as shown by the intensity profiles. Most critically, LS addition significantly increased the intracellular uptake of MK2i, as shown by flow cytometry on isolated cells 1 h after aorta treatment (Fig. 2G).

PPAA and similar polymers have been shown to significantly increase cell internalization of MK2i and similar peptides *in vitro*, with the hydrophobic side group of the polymer being critical in interaction with cell membranes and, combined with the carboxylic acid group, promoting pH-dependent escape from endolysosomal vesicles [27]. Here, we also probed the importance of the PPAA structure in tissue-level cell internalization relative to use of other analogous polyanions in the LbL balloon coating (Fig. S2). PPAA was compared to poly(acrylic acid) (PAA), a negatively charged polymer that lacks the hydrophobic propyl side chain present on PPAA. While PAA also effectively loaded and released MK2i from the balloons, cell internalization of MK2i delivered into rat aortas with PAA + LS DCBs was negligible compared to the significant uptake realized in tissues treated with PPAA-based + LS DCBs. These data confirm the criticality of the use of PPAA in the LbL DCB design.

Comparison to topical MK2i-NP delivery.

We next sought to benchmark the relative intracellular delivery of convective and DCB approaches with an in-house gold standard. To accomplish this, cell uptake of MK2i was compared to our previously established method of topical, solution-based MK2i-NP delivery to explanted vascular tissues [12]. We previously showed that a 30 min incubation with MK2i-NPs at concentrations of 10 μM and 50 μM MK2i-NPs prevented IH and SMC phenotype switching in venous tissues and in cell culture studies *in vitro* [12,13]. To compare to an established benchmark, the intracellular delivery of MK2i peptide achieved by the new intravascular delivery approaches was compared to that achieved by topical treatment with 10 and 50 μM MK2i-NPs for 30 min. It was found that all of the 3-min convective and DCB delivery approaches tested yielded levels of intracellular delivery that fall within the range of uptake achieved by the 30 min 10–50 μM topical MK2i-NP

treatment (Fig. S3). Importantly the +LS DCB method achieved levels of intracellular delivery within the aortic tissue that matched that of the 50 μM MK2i-NPs, a concentration recently used in successful rabbit vascular transplant studies [12].

Pharmacokinetics of MK2i administered by convection and DCB.

To study the arterial retention of MK2i over time under flow, a bioreactor was constructed to maintain the aortas under physiological conditions (Fig. 3A, S4). The viability of aortas housed in this bioreactor was confirmed at 24 h and 7 day time points using the MTT viability assay, with no significant drop in viability after one week (Fig. 3B). Initial tissue MK2i concentration was calculated from digested aortas immediately after treatment (Fig. 3C). Using this bioreactor setup, the amount of MK2i in the vessel wall was visualized at 24 h post-treatment for all delivery strategies and formulations (Fig. 3D) and quantified from digested tissues (Fig. 3E, S5A). Convection with MK2i-NPs and +LS DCBs both had significantly more retention at 24 h than the other delivery formulations. Therefore, these two lead delivery methods were assessed for longer-term MK2i retention at 3 days and 7 days in the flow loop bioreactor. MK2i was still present within the arterial wall at these later time points (Fig. 3F). Tissue MK2i concentration decreased over time, but a significant quantify of peptide was retained within the tissue (Fig. 3G, S5B). MK2i presence up to 7 days is important for inhibition of the acute stress response, as it has been shown that the majority of cellular proliferation takes place within the first week after vascular interventions [35,36]. Interestingly, though MK2i delivery from +LS DCBs is concentrated on the lumen-side of the arterial wall after initial delivery, intensity profiles of the aortas at different time points show that the delivered MK2i disperses homogeneously throughout the vessel wall over time (Fig. S6). After 24 h, there is still a slight gradient of MK2i, but after 3d, the MK2i is evenly dispersed throughout the vessel, similar to the MK2i dispersion seen with convective delivery.

MK2i blocks phosphorylation of CREB over time in treated rat aortas.

The ability of delivered MK2i to block MK2 signaling was determined by measuring the downstream phosphorylation of direct MK2 substrate cAMP response element–binding protein (CREB) [37], a transcription factor involved in VSMC proliferation [38,39]. To measure inhibition of acute CREB phosphorylation, each rat aorta was divided in half – one half was balloon damaged and vehicle treated while the other half was balloon damaged and then treated with MK2i + PPAA formulations. After 1 h static incubation, tissue lysates were prepared and levels of P-CREB were analyzed by Western blot (Fig. 4A and B). The relative level of P-CREB induced by balloon damage was significantly reduced in convective MK2i-NP treated and +LS DCB treated aortas and was similar to the level in a control untreated, undamaged aorta (Fig. 4A). Pairwise comparisons of aorta halves showed that balloon damage significantly increased P-CREB levels compared to an untreated, undamaged aortic segment, and treatment with MK2i-NPs or + LS DCB inhibited that P-CREB induction (Fig. 4B). The inclusion of LS in the DCB formulation has an obvious beneficial effect on MK2i delivery and bioactivity, and therefore DCB formulations in studies from this point will only use + LS forms and will be referred to as “MK2i DCBs”.

The pharmacodynamics of MK2 signaling inhibition were next monitored over time. To measure MK2i activity after incubation in the flow loop, untreated or MK2i-treated aortas were divided in half – one half was stimulated with lysophosphatidic acid (LPA), which has been shown to stimulate VSMC CREB phosphorylation in previous studies [12,40], while the other half was left unstimulated. The amount of P-CREB induction was compared between the two halves for each treatment group at 24 h (Fig. 4C), 3 days (Fig. 4D, S7A), and 7 days (Fig. 4E, S7B). LPA was shown to stimulate an increase in P-CREB in the untreated samples at each time point, while MK2i-NP and MK2i DCB treatment effectively blocked LPA-stimulated CREB phosphorylation at all time points, having no significant difference in P-CREB levels from samples not stimulated with LPA. These results show the potent effect of intravascular MK2i + PPAA delivery on MK2 inhibition and corroborates that the MK2i peptide that was observed in the artery after 7 days in dynamic culture remained bioactive.

MK2i treatment inhibits proliferation and fibrosis *ex vivo*.

Effects of MK2i treatment were analyzed by incubating rat aortas in the flow loop bioreactor for 7 days. Using PCNA as a marker for proliferating cells, it was observed that balloon damage led to a significant increase in proliferating medial cells after 7 days. Convectively delivered MK2i-NPs and MK2i DCB treatment decreased the percentage of PCNA positive cells in the media layer, with the MK2i DCB trending toward a modestly more potent effect (Fig. 5). Balloon damaged aortas expressed significantly more fibronectin throughout the media layer, which is a characteristic of the synthetic smooth muscle cell phenotype [41], while MK2i-NP and MK2i DCB treated aortas maintained low expression of fibronectin, similar to fresh, nondamaged tissue samples (Fig. 5).

MK2i preserves vessel contractility *ex vivo*.

Preservation of the healthy contractile SMC phenotype is essential to preventing IH development and restenosis after balloon injury. Balloon damage significantly decreased expression of contractile proteins transgelin (SM22) and myosin heavy chain (MYH), while MK2i treated aortas maintained the healthy SMC phenotype by preserving expression of these contractile proteins (Fig. 6A and B). It is important to note that CD31 staining of balloon damaged aortas showed no endothelial coverage after 7 days (Fig. S8). This confirms that balloon damage denudes the endothelial lining of the aortas, and that re-endothelialization does not occur after 7d in the flow loop bioreactor.

As a functional readout of blocking SMC phenotype switching, the contractile responses of untreated, treated, and damaged aortas to phenylephrine (PE), a SMC specific agonist, were compared after 3d in the flow loop bioreactor. Aorta segments were hung in a muscle bath (Fig. 6C) and treated with a series of dilutions of PE. Fig. 6D shows that balloon damage in the absence of treatment resulted in a loss of SMC-specific vessel contraction. MK2i-NP convective treatment and MK2i DCB treatment both preserved SMC contractile force to levels similar to that of the 3d incubated, untreated, undamaged control arteries. Since the MTT assay confirmed viability, these data suggest that balloon injury leads to loss of contractile function that is not due to cell death. Therefore, MK2i-NP and MK2i DCB

treatment effectively prevent SMCs from switching to the synthetic phenotype and losing contractility.

MK2i DCB treatment blocks IH in an *in vivo* rat carotid artery balloon injury model.

To assess the ability of MK2i DCBs to block IH development after balloon injury, an *in vivo* rat carotid artery balloon injury model was employed. Previous studies have shown that rat carotid artery balloon injury consistently results in neointima formation by 14 days after the intervention [33,42–46]. Because the convective treatment is difficult to employ *in vivo* in rodents, these studies focused on the DCB strategy.

Carotid angioplasty was performed, and arteries were then either left untreated or treated with a follow-up application of the DCB at the site of injury (Fig. 7A). The MK2i peptide could be visualized in the MK2i DCB treated arteries at 14 days after injury (Fig. S9). Angioplasty caused significant neointima formation, whereas MK2i DCB treatment inhibited IH (Fig. 7B) and reduced the intima/media ratio (Fig. 7F). Importantly, it was observed that MK2i DCB treatment did not impair vessel re-endothelialization (Fig. 7C) as seen with paclitaxel balloons in other studies [47,48]. Furthermore, MK2i DCB treatment inhibited macrophage infiltration (Fig. 7D, G) and T cell recruitment (Fig. 7E, G) induced by angioplasty, both of which contribute to intimal thickening [49–51].

MK2i DCB treatment was shown to maintain on-target MK2 inhibition as measured by tissue levels of P-CREB (Fig. S10) and likewise to block SMC phenotype switching at the site of the angioplasty. MK2i DCB treatment inhibited proliferation (Fig. 8A, E), fibronectin (Fig. 8B, E), and vimentin (Fig. 8C, E), all hallmarks of the synthetic phenotype [7,8, 52,53]. Conversely, MK2i DCB treatment preserved expression of the contractile phenotype marker SM22 (Fig. 8D and E). Additionally, neointima layers of untreated arteries had visually denser collagen networks than the neointima of MK2i DCB treated arteries as shown with Gomori trichrome (Fig. 7B, S11), indicating MK2i inhibits development of mature IH by preventing SMCs from switching to the ECM-producing synthetic phenotype. These results suggest that MK2i DCBs may represent an ideal therapeutic option that blocks SMC phenotype switching, inflammation, and neointima formation, while allowing endothelial repair after angioplasty.

4. Discussion

These studies establish that both convective and DCB approaches to intravascular delivery of MK2i + PPAA have the potential to prevent restenosis after angioplasty. Both methods achieve successful MK2i delivery to *ex vivo* aortas (Figs. 1 and 2) and are retained within the arteries for up to 7 days post-treatment (Fig. 3). MK2i DCB treatment and convective delivery of MK2i-NPs performed similarly in the *ex vivo* model studies. Despite having different delivery profiles initially (Figs. 1D and 2F), total MK2i concentration and retention over time were very similar.

Analogous to previously successful methods of *ex vivo* MK2i-NP treatment during vessel bypass grafting procedures [12,13], convective delivery of MK2i-NPs and MK2i DCB delivery both achieve therapeutically relevant MK2i concentrations within the tissue (Fig.

S3). Pharmacodynamic studies showed that both delivery methods significantly inhibited CREB phosphorylation at all time points over 7 days in the dynamic culture bioreactor (Fig. 4), and MK2i DCB treatment had sustained P-CREB inhibition after 14 days *in vivo* (Fig. S10), suggesting that MK2 inhibitory activity is sustained in the tissue for at least two weeks. Potent MK2 inhibition over the first two weeks protects the tissue in the critical, acute stages post-injury and is anticipated to potentially yield long-term inhibition of restenosis. The majority of cellular proliferation occurs within the first week after interventional vascular procedures [35,36], and inflammation has been determined to peak around 3 days post-injury [54,55]. This early proliferation and inflammation coincide with the SMC phenotype switch [56], and by targeting a node that blocks this switch in the acute stage post-angioplasty, we contend that it will reduce the secretion of matrix and neointimal growth that drive restenosis progression. We showed that both MK2i-NP convective delivery and MK2i DCB treatments successfully mitigated hallmark signs of phenotype switching, including cell proliferation, fibrosis, and loss of contractile protein presence and function (Figs. 5 and 6).

While convective and DCB treatments were generally similar, the DCB approach proved superior in some SMC phenotype-related readouts at longer time points. Both methods robustly blocked vessel fibrosis and fibronectin production (Fig. 5B). Though both routes of administration significantly decreased cellular proliferation relative to the untreated, balloon damaged arteries, the MK2i DCB treatment had a more potent effect than MK2i-NP convective delivery (Fig. 5A). IHC for contractile markers SM22 and MYH also showed that MK2i DCB had a significant effect on maintaining contractile protein expression, with levels similar to healthy control arteries and statistically different from the untreated, balloon damaged arteries. MK2i-NPs also preserved the contractile phenotype, but it was more modest and not significant compared to untreated aortas (Fig. 6).

The differences between DCB and convective MK2i-NP performance can potentially be attributed to multiple factors. First, it has been observed in porous balloons that high pressure injection into the vessel wall can cause tissue damage [57]. It is possible that pressurization and forcing fluid flow into the wall of the vessel contribute to vessel damage beyond that caused by the angioplasty procedure itself. Additionally, the delivery profiles of the MK2i DCBs show that the majority of the delivered MK2i is initially concentrated near the luminal surface. This spatially co-localizes with the region where SMCs of the vessel wall are more damaged by balloon injury, whereas convective delivery yields more homogeneous dispersion of the MK2i throughout the vessel wall immediately following treatment. Shear stress has been shown to be a factor in SMC phenotype switching [58], so the SMCs adjacent to the lumen may be important to target early after injury due to the denudation of the endothelium that occurs at the angioplasty site.

The advantages of the MK2i DCBs observed in *ex vivo* rat aorta studies motivated our focus on this delivery platform for testing in the *in vivo* rat carotid balloon injury model. There is also a stronger clinical precedent for DCB use than there is for convective delivery approaches. Treatment with the MK2i DCB effectively inhibited neointima formation in damaged rat carotids after 14 days (Fig. 7), whereas untreated balloon damaged arteries had noticeable neointima formation in all samples. Additionally, MK2i DCBs blocked cellular

proliferation of medial SMCs, reduced immune cell infiltration, and moderated vessel fibrosis, while preserving the contractile SMC phenotype within the medial layer of the arteries. Vessels treated with MK2i DCB were also re-endothelialized, suggesting that the arteries reached a healthy steady state condition post-angioplasty. Early re-endothelialization may also contribute to the reduction in IH observed in the treated vessels. In sum, these data suggest that MK2i DCB's treatment is associated with multiple mechanisms that prevent IH and promote vessel patency.

Current DCBs in use in the clinic employ proliferation blockers such as paclitaxel and sirolimus. These drugs are effective in preventing restenosis over naked balloon angioplasty, especially in coronary artery disease [59]. However, these DCBs have issues with primary patency and amputation at 1 year in peripheral artery restenosis [11,60], as one study showed only 58.1% primary patency of vessels one year after paclitaxel DCB treatment [61]. These results suggest a strong need for improved balloon treatments in the peripheral arterial circulation. We hypothesize that one of the shortcomings of current DCBs is that they only target cellular proliferation. These drugs can also inhibit vessel re-endothelialization [10], which is important for preventing thrombosis and IH. Critically, these drugs fail to inhibit the underlying signaling pathways and SMC phenotype switch that drive IH progression. On the other hand, MK2 inhibition reduces inflammation, ECM production, and SMC phenotype switching without inhibiting re-endothelialization (Fig. 7C), all of the key facets known to contribute to neointima formation [62,46,63].

Previous RNA sequencing data on primary human coronary artery SMCs showed that MK2 inhibition leads to broad changes in genetic expression that helps to maintain the SMC contractile phenotype [12]. MK2i inhibition resulted in a significant decrease in many proinflammatory genes, leading to decreased inflammatory cell recruitment seen here *in vivo* (Fig. 7D and E), and maintenance of multiple genes associated with contractile proteins, thus preserving VSMC contractility (Fig. 6D) and expression of contractile phenotype proteins (Fig. 8D). We can conclude that genetic changes in SMCs leading to phenotype switching is caused by activation of the "stress-activated" P38-MK2 signaling pathway, which converges downstream to modulate transcription factors such as CREB that regulate genes related to VSMC phenotype [64]. MK2 also phosphorylates hrRNP A0 and TTP, proteins that stabilize and increase translation of the mRNA of pro-inflammatory genes [65,66]. By blocking these effectors of the p38-MK2 pathway, MK2i prevents broad genetic changes and subsequent inflammation and phenotype switching in VSMCs, leading to reduced IH after injury.

These studies mark, to our knowledge, the first use of DCBs and pressure-based delivery for intravascular administration of intracellularly-acting peptides. Previous DCB studies have explored LbL, multilayer spray coating, and hydrogel-based surface loading of anti-restenosis drugs such as everolimus and have also explored spray coating balloons with a combination of miRNA and the polymers polyethyleneimine/polyacrylic acid (PEI/PAA) [62,26,67]. However, these approaches required more complex formulations such as hydrogels, liposomes, or polymeric nanoparticles to effectively load their cargo. The cationic layers of the MK2i DCBs comprise solely the therapeutic molecule MK2i, simplifying the coating process and improving drug loading. While electrostatic coating was used, the

miRNA work still utilized an anionic carrier polymer (PAA) versus solely loading the anionic therapeutic miRNA. Additionally, in our work, the PPAA + LS as the anionic layer helps to promote tissue penetration and endosome escape for intracellular delivery of the MK2i cargo. In sum, the simplicity and multifunctionality of the MK2i DCB design, along with its promising therapeutic efficacy, make it promising for clinical translation.

5. Conclusions

Two viable methods were realized for intravascular delivery of MK2i + PPAA to prevent IH and restenosis after peripheral angioplasty. Both convection of MK2i-NP solutions and layer-by-layer coated DCBs successfully achieved transfer of MK2i + PPAA to the arterial wall and maintained MK2i activity 7 days post-administration. Extended retention of MK2i decreased MK2 kinase activity and consequently SMC proliferation and ECM deposition, while maintaining contractile VSMC gene expression and function in *ex vivo* rat aorta. MK2i DCB treatment also effectively inhibited inflammation, SMC phenotype switching, and neointima formation 14 days post-angioplasty *in vivo*. As opposed to current methods of restenosis prevention such as paclitaxel coated balloons that only target cellular proliferation, MK2i + PPAA treatment offers a holistic approach to blocking IH development by targeting inflammation and SMC phenotype switching while allowing endothelial repair. These collective results suggest that MK2i DCBs are a promising new approach for improving patency post-angioplasty.

Future studies will explore the effectiveness of MK2i DCB treatment in diseased arteries after angioplasty, as the presence of atherosclerotic plaque may affect the transfer of MK2i from the balloon surface. Additionally, we plan to test this treatment method in larger animal models, such as pigs, which will allow balloon deployment at common sites of peripheral angioplasty, such as the femoral and iliac arteries.

Study approval

All animal studies were approved by the Vanderbilt University Institutional Animal Care and Use Committee and conformed to the Guide for the Care and Use of Laboratory Animals.

Supplementary Material

Refer to Web version on PubMed Central for supplementary material.

Acknowledgements

This work was supported by the NIH NHLBI (R01HL122347 and F31HL162476). We acknowledge the Translational Pathology Shared Resource supported by NCI/NIH Cancer Center Support Grant P30CA068485. We also acknowledge the lab of Tonia Rex at Vanderbilt for the use of their cryostat and the Vanderbilt Institute for Nanoscale Science and Engineering (VINSE) for the use of the SEM. Schematics were made using BioRender.

Data availability

Data will be made available on request.

References

[1]. Sobolevskaya EV, Shumkov OA, Smagin MA, Guskov AE, Malysheva AV, Atuchin VV, Nimaev VV, Markers of restenosis after percutaneous transluminal balloon angioplasty in patients with critical limb ischemia, Int. J. Mol. Sci 24 (10) (2023).

[2]. Early M, Kelly DJ, The consequences of the mechanical environment of peripheral arteries for nitinol stenting, Med. Biol. Eng. Comput 49 (11) (2011) 1279–1288. [PubMed: 21833628]

[3]. Scheinert D, Scheinert S, Sax J, Piorkowski C, Braunlich S, Ulrich M, Biamino G, Schmidt A, Prevalence and clinical impact of stent fractures after femoropopliteal stenting, J. Am. Coll. Cardiol 45 (2) (2005) 312–315. [PubMed: 15653033]

[4]. Shaikh F, Maddikunta R, Djelmami-Hani M, Solis J, Allaqaband S, Bajwa T, Stent fracture, an incidental finding or a significant marker of clinical in-stent restenosis? Cathet. Cardiovasc. Interv 71 (5) (2008) 614–618.

[5]. Schillinger M, Minar E, Restenosis after percutaneous angioplasty: the role of vascular inflammation, Vasc. Health Risk Manag 1 (1) (2005) 73–78. [PubMed: 17319099]

[6]. Pourmoussa AJ, Smuclovisky E, Peña C, Katzen B, Maximizing Angioplasty Results in Peripheral Interventions, Techniques in Vascular and Interventional Radiology, 2022.

[7]. Louis SF, Zahradka P, Vascular smooth muscle cell motility: from migration to invasion, Experimental and Clinical Cardiology, Pulsus Group (2010) e75.

[8]. Tang HY, Chen AQ, Zhang H, Gao XF, Kong XQ, Zhang JJ, Vascular smooth muscle cells phenotypic switching in cardiovascular diseases, Cells 11 (24) (2022).

[9]. Byrne RA, Joner M, Kastrati A, Byrne RA, Joner M, Alfonso F, Kastrati A, Drug-coated balloon therapy in coronary and peripheral artery disease, Nat. Rev. Cardiol (2014) 13–23. [PubMed: 24189405]

[10]. Hayashi SI, Yamamoto A, You F, Yamashita K, Ikegame Y, Tawada M, Yoshimori T, Shimizu S, Nakashima S, The stent-eluting drugs sirolimus and paclitaxel suppress healing of the endothelium by induction of autophagy, Am. J. Pathol 175 (2009) 2226–2234. [PubMed: 19815708]

[11]. Ipema J, Huizing E, Schreve MA, De Vries J-PPM, Ünlü Ç, Editor's choice – drug coated balloon angioplasty vs. Standard percutaneous transluminal angioplasty in below the knee peripheral arterial disease: a systematic review and meta-analysis, Eur. J. Vasc. Endovasc. Surg 59 (2) (2020) 265–275. [PubMed: 31889657]

[12]. Tierney JW, Evans BC, Cheung-Flynn J, Wang B, Colazo JM, Polcz ME, Cook RS, Brophy CM, Duvall CL, Therapeutic MK2 inhibition blocks pathological vascular smooth muscle cell phenotype switch, JCI Insight 6 (2021) e142339. [PubMed: 34622803]

[13]. Evans BC, Hocking KM, Osgood MJ, Voskresensky I, Dmowska J, Kilchrist KV, Brophy CM, Duvall CL, MK2 inhibitory peptide delivered in nanopolyplexes prevents vascular graft intimal hyperplasia, Sci. Transl. Med (2015) 1–12.

[14]. Mukalel AJ, Evans BC, Kilchrist KV, Dailing EA, Burdette B, Cheung-Flynn J, Brophy CM, Duvall CL, Excipients for the lyoprotection of MAPKAP kinase 2 inhibitory peptide nano-polyplexes, in: Journal of Controlled Release, Elsevier BV, 2018, pp. 110–119.

[15]. Kilchrist KV, Evans BC, Brophy CM, Duvall CL, Mechanism of enhanced cellular uptake and cytosolic retention of MK2 inhibitory peptide nano-polyplexes. Cellular and Molecular Bioengineering, Springer New York LLC, 2016, pp. 368–381.

[16]. Evans BC, Hocking KM, Kilchrist KV, Wise ES, Brophy CM, Duvall CL, Endosomolytic nano-polyplex platform Technology for cytosolic peptide delivery to inhibit pathological vasoconstriction, ACS Nano (2015) 5893–5907. [PubMed: 26004140]

[17]. Evans BC, Fletcher RB, Kilchrist KV, Dailing EA, Mukalel AJ, Colazo JM, Oliver M, Cheung-Flynn J, Brophy CM, Tierney JW, Isenberg JS, Hankenson KD, Ghimire K, Lander C, Gersbach CA, Duvall CL, An anionic, endosome-escaping polymer to potentiate intracellular delivery of cationic peptides, biomacromolecules, and nanoparticles, Nat. Commun 10 (2019) 1–19. [PubMed: 30602773]

[18]. Decker JA, Helmer M, Bette S, Schwarz F, Kroencke TJ, Scheurig-Muenkler C, Comparison and trends of endovascular, surgical and hybrid revascularizations and the influence of comorbidity in

1 million hospitalizations due to peripheral artery disease in Germany between 2009 and 2018, Cardiovasc. Intervent. Radiol 45 (10) (2022) 1472–1482. [PubMed: 35428938]

[19]. Westedt U, Barbu-Tudoran L, Schaper AK, Kalinowski M, Alfke H, Kissel T, Deposition of nanoparticles in the arterial vessel by porous balloon catheters: localization by confocal laser scanning microscopy and transmission electron microscopy, AAPS PharmSci 4 (4) (2002) 206–211.

[20]. Oberhoff M, Kunert W, Herdeg C, Küttner A, Kranzhöfer A, Horch B, Baumbach A, Karsch KR, Oberhoff M, Baumbach A, Karsch KR, Kunert W, Herdeg C, Küttner A, Kranzhöfer A, Horch B, Inhibition of smooth muscle cell proliferation after local drug delivery of the antimitotic drug paclitaxel using a porous balloon catheter, Basic Res. Cardiol (2001) 275–282. [PubMed: 11403421]

[21]. Mann MJ, Whittemore AD, Donaldson MC, Belkin M, Conte MS, Polak JF, Orav EJ, Ehsan A, Dell'Acqua G, Dzau VJ, Ex-vivo gene therapy of human vascular bypass grafts with E2F decoy: the PREVENT single-centre, randomised, controlled trial, Lancet 354 (9189) (1999) 1493–1498. [PubMed: 10551494]

[22]. Bunch F, Nair P, Aggarwala G, Dippel E, Kassab E, Khan MA, Lecroy C, McClure JM, Tolleson T, Walker C, A universal drug delivery catheter for the treatment of infrapopliteal arterial disease using liquid therapy, Cathet. Cardiovasc. Interv 96 (2) (2020) 393–401.

[23]. Bunch F, Walker C, Kassab E, Carr J, A universal drug delivery catheter for the treatment of infrapopliteal arterial disease: results from the multi-center first-in-human study, Cathet. Cardiovasc. Interv 91 (2) (2018) 296–301.

[24]. Atigh MK, Turner E, Christians U, Yazdani SK, The Use of an Occlusion Perfusion Catheter to Deliver Paclitaxel to the Arterial Wall, Cardiovascular Therapeutics, 2017, pp. 1–9.

[25]. Udofot O, Lin LH, Thiel WH, Erwin M, Turner E, Miller FJ, Giangrande PH, Yazdani SK, Delivery of cell-specific aptamers to the arterial wall with an occlusion perfusion catheter. Molecular Therapy - Nucleic Acids, Cell Press, 2019, pp. 360–366.

[26]. Iyer R, Kuriakose AE, Yaman S, Su L-C, Shan D, Yang J, Liao J, Tang L, Banerjee S, Xu H, Nguyen KT, Nanoparticle eluting-angioplasty balloons to treat cardiovascular diseases, Int. J. Pharm 554 (2019) 212–223. [PubMed: 30408532]

[27]. Evans BC, Fletcher RB, Kilchrist KV, Dailing EA, Mukalel AJ, Colazo JM, Oliver M, Cheung-Flynn J, Brophy CM, Tierney JW, Isenberg JS, Hankenson KD, Ghimire K, Lander C, Gersbach CA, Duvall CL, An anionic, endosome-escaping polymer to potentiate intracellular delivery of cationic peptides, biomacromolecules, and nanoparticles. Nature Communications, Nature Publishing Group, 2019, pp. 1–19.

[28]. Ferritto M, Tirrell DA, POLY(2-ETHYLACRYLIC ACID), Macromolecular Synthesis, Wiley, New York, 1992, pp. 59–62.

[29]. Convertine AJ, Benoit DSW, Duvall CL, Hoffman AS, Stayton PS, Development of a novel endosomolytic diblock copolymer for siRNA delivery, J. Contr. Release (2009) 221–229.

[30]. Wang J, Kural MH, Wu J, Leiby KL, Mishra V, Lysyy T, Li G, Luo J, Greaney A, Tellides G, Qyang Y, Huang N, Niklason LE, An ex vivo physiologic and hyperplastic vessel culture model to study intra-arterial stent therapies, Biomaterials 275 (2021) 120911. [PubMed: 34087584]

[31]. Cunningham KS, Gotlieb AI, The role of shear stress in the pathogenesis of atherosclerosis, Lab. Invest 85 (1) (2005) 9–23. [PubMed: 15568038]

[32]. Wise ES, Hocking KM, Eagle S, Absi T, Komalavilas P, Cheung-Flynn J, Brophy CM, Preservation solution impacts physiologic function and cellular viability of human saphenous vein graft, Surgery 158 (2) (2015) 537–546. [PubMed: 26003912]

[33]. Tulis DA, Rat Carotid Artery Balloon Injury Model, Humana Press2007, pp. 1–30.

[34]. Dailing EA, Kilchrist KV, Tierney JW, Fletcher RB, Evans BC, Duvall CL, Modifying cell membranes with anionic polymer amphiphiles potentiates intracellular delivery of cationic peptides, in: ACS Applied Materials and Interfaces, American Chemical Society, 2020, pp. 50222–50235.

[35]. Kalra M, Miller VM, Early remodeling of saphenous vein grafts: proliferation, migration and apoptosis of adventitial and medial cells occur simultaneously with changes in graft diameter and blood flow, J. Vasc. Res (2000) 576–584. [PubMed: 11146412]

[36]. Durand E, Mallat Z, Addad F, Vilde F, Desnos M, Guerot C, Tedgui A, Lafont A, Time courses of apoptosis and cell proliferation and their relationship to arterial remodeling and restenosis after angioplasty in an atherosclerotic rabbit model, J. Am. Coll. Cardiol 39 (10) (2002) 1680–1685. [PubMed: 12020497]

[37]. Johannessen M, Moens U, Multisite Phosphorylation of the cAMP Response Element-Binding Protein (CREB) by a Diversity of Protein Kinases Human Polyomaviruses and Papillomaviruses View Project SLE and Anti-dsDNA Antibodies View Project, 2007.

[38]. Nakanishi K, Saito Y, Azuma N, Sasajima T, Cyclic adenosine monophosphate response-element binding protein activation by mitogen-activated protein kinase-activated protein kinase 3 and four-and-a-half LIM domains 5 plays a key role for vein graft intimal hyperplasia, in: Journal of Vascular Surgery, Mosby Inc., 2013, pp. 182–193, 193.e1–10.

[39]. Lee GL, Chang YW, Wu JY, Wu ML, Wu KK, Yet SF, Kuo CC, TLR 2 induces vascular smooth muscle cell migration through cAMP response element-binding protein-mediated interleukin-6 production, Arterioscler. Thromb. Vasc. Biol (2012) 2751–2760. [PubMed: 22995520]

[40]. Lee CW, Nam JS, Park YK, Choi HK, Lee JH, Kim NH, Cho J, Song DK, Suh HW, Lee J, Kim YH, Huh SO, Lysophosphatidic acid stimulates CREB through mitogen- and stress-activated protein kinase-1. Biochemical and Biophysical Research Communications, Academic Press Inc., 2003, pp. 455–461.

[41]. Jain M, Dhanesha N, Doddapattar P, Chorawala MR, Nayak MK, Cornelissen A, Guo L, Finn AV, Lentz SR, Chauhan AK, Smooth muscle cell-specific fibronectin-EDA mediates phenotypic switching and neointimal hyperplasia, J. Clin. Invest 130 (2020) 295–314. [PubMed: 31763999]

[42]. Zheng SS, Zhao J, Chen JW, Shen XH, Hong XL, Fu GS, Fu JY, Inhibition of neointimal hyperplasia in balloon-induced vascular injuries in a rat model by miR-22 loading Laponite hydrogels, Biomater. Adv 142 (2022) 213140. [PubMed: 36228507]

[43]. Liu Z, Wu C, Zou X, Shen W, Yang J, Zhang X, Hu X, Wang H, Liao Y, Jing T, Exosomes derived from mesenchymal stem cells inhibit neointimal hyperplasia by activating the Erk1/2 signalling pathway in rats, Stem Cell Res. Ther 11 (1) (2020) 220. [PubMed: 32513275]

[44]. Burke-Kleinman J, Rubianto J, Hou G, Santerre JP, Bendeck MP, Matrix-binding N-Cadherin–Targeting chimeric peptide inhibits intimal thickening but not endothelial repair in balloon-injured carotid arteries, Arterioscler. Thromb. Vasc. Biol 43 (9) (2023) 1639–1652. [PubMed: 37409527]

[45]. Gao M, Gao X, Taniguchi R, Brahmandam A, Matsubara Y, Liu J, Liu H, Zhang W, Dardik A, Sex differences in arterial identity correlate with neointimal hyperplasia after balloon injury, Mol. Biol. Rep 49 (9) (2022) 8301–8315. [PubMed: 35715609]

[46]. Wang W, Zhang Y, Hui H, Tong W, Wei Z, Li Z, Zhang S, Yang X, Tian J, Chen Y, The effect of endothelial progenitor cell transplantation on neointimal hyperplasia and reendothelialisation after balloon catheter injury in rat carotid arteries, Stem Cell Res. Ther 12 (1) (2021) 99. [PubMed: 33536065]

[47]. Axel DI, Kunert W, Goggelmann C, Oberhoff M, Herdeg C, Kuttner A, Wild DH, Brehm BR, Riessen R, Koveker G, Karsch KR, Paclitaxel inhibits arterial smooth muscle cell proliferation and migration in vitro and in vivo using local drug delivery, Circulation 96 (2) (1997) 636–645. [PubMed: 9244237]

[48]. Coomber BL, Gotlieb AI, In vitro endothelial wound repair, Arterioscler. Thromb. Vasc. Biol 10 (2) (1990) 215–222.

[49]. Davies MG, Hagen P-O, Pathobiology of intimal hyperplasia, Br. J. Surg 81 (1994) 1254–1269. [PubMed: 7953384]

[50]. Deglise S, Bechelli C, Allagnat F, Vascular smooth muscle cells in intimal hyperplasia, an update, Front. Physiol 13 (2022) 1081881. [PubMed: 36685215]

[51]. Bai H, Wang Z, Li M, Sun P, Wei S, Wang W, Wang Z, Xing Y, Li J, Dardik A, Inhibition of programmed death-1 decreases neointimal hyperplasia after patch angioplasty, J. Biomed. Mater. Res. B Appl. Biomater 109 (2) (2021) 269–278. [PubMed: 32770622]

[52]. Jain M, Dhanesha N, Doddapattar P, Chorawala MR, Nayak MK, Cornelissen A, Guo L, Finn AV, Lentz SR, Chauhan AK, Smooth muscle cell-specific fibronectin-EDA mediates phenotypic

switching and neointimal hyperplasia, J. Clin. Invest (2020) 295–314. American Society for Clinical Investigation.

[53]. Rensen SSM, Doevendans PAFM, Van Eys GJJM, Regulation and Characteristics of Vascular Smooth Muscle Cell Phenotypic Diversity, Netherlands Heart Journal, 2007, pp. 100–108. Bohn Stafleu van Loghum.

[54]. Cai J, Yuan H, Wang Q, Yang H, Al-Abed Y, Hua Z, Wang J, Chen D, Wu J, Lu B, Pribis JP, Jiang W, Yang K, Hackam DJ, Tracey KJ, Billiar TR, Chen AF, HMGB1-Driven inflammation and intimal hyperplasia after arterial injury involves cell-specific actions mediated by TLR4, Arterioscler. Thromb. Vasc. Biol 35 (12) (2015) 2579–2593. [PubMed: 26515416]

[55]. Bu DX, Erl W, De Martin R, Hansson GK, Yan ZQ, IKKβ-dependent NF-κB pathway controls vascular inflammation and intimal hyperplasia, Faseb. J 19 (10) (2005) 1293–1295. [PubMed: 15939736]

[56]. Melnik T, Jordan O, Corpataux JM, Delie F, Saucy F, Pharmacological prevention of intimal hyperplasia: a state-of-the-art review, Pharmacol. Ther 235 (2022) 108157. [PubMed: 35183591]

[57]. Herdeg C, Oberhoff M, Baumbach A, Haase KK, Horch B, Kranzhoefer A, Karsch KR, Local drug delivery with porous balloons in the rabbit: assessment of vascular injury for an improvement of application parameters, Cathet. Cardiovasc. Diagn 41 (3) (1997) 308–314. [PubMed: 9213030]

[58]. Jensen LF, Bentzon JF, Albarran-Juarez J, The phenotypic responses of vascular smooth muscle cells exposed to mechanical cues, Cells 10 (9) (2021).

[59]. Rittger H, Brachmann J, Sinha AM, Waliszewski M, Ohlow M, Brugger A, Thiele H, Birkemeyer R, Kurowski V, Breithardt OA, Schmidt M, Zimmermann S, Lonke S, von Cranach M, Nguyen TV, Daniel WG, Wohrle J, A randomized, multicenter, single-blinded trial comparing paclitaxel-coated balloon angioplasty with plain balloon angioplasty in drug-eluting stent restenosis: the PEPCAD-DES study, J. Am. Coll. Cardiol 59 (15) (2012) 1377–1382. [PubMed: 22386286]

[60]. Mori M, Sakamoto A, Kawakami R, Sato Y, Jinnouchi H, Kawai K, Cornelissen A, Virmani R, Finn AV, Paclitaxel- and sirolimus-coated balloons in peripheral artery disease treatment: current perspectives and concerns, Vascular and Endovascular Review 4 (2021).

[61]. Phair J, Carnevale M, Lipsitz EC, Shariff S, Scher L, Garg K, Amputation-free survival in patients with critical limb ischemia treated with paclitaxel-eluting stents and paclitaxel-coated balloons, Ann. Vasc. Surg 62 (2020) 8–14. [PubMed: 31207400]

[62]. Fu J-Y, Lai Y-X, Zheng S-S, Wang J, Wang Y, Ren K, Yu L, Fu G, Ji J, Mir-22-incorporated polyelectrolyte coating prevents intima hyperplasia after balloon-induced vascular injury, Biomater. Sci (2022).

[63]. Zhao J, Fu J.y., Jia F, Li J, Yu B, Huang Y, Ren K.f., Ji J, Fu G.s., Precise regulation of inflammation and oxidative stress by ROS-responsive prodrug coated balloon for preventing vascular restenosis, Adv. Funct. Mater 33 (30) (2023).

[64]. Ono H, Ichiki T, Fukuyama K, Iino N, Masuda S, Egashira K, Takeshita A, cAMP-response element-binding protein mediates tumor necrosis factor-alpha-induced vascular smooth muscle cell migration, Arterioscler. Thromb. Vasc. Biol (2004) 1634–1639. [PubMed: 15242860]

[65]. Rousseau S, Inhibition of SAPK2a/p38 prevents hnRNP A0 phosphorylation by MAPKAP-K2 and its interaction with cytokine mRNAs, EMBO J. 21 (23) (2002) 6505–6514. [PubMed: 12456657]

[66]. Ronkina N, Menon MB, Schwermann J, Tiedje C, Hitti E, Kotlyarov A, Gaestel M, MAPKAP kinases MK2 and MK3 in inflammation: complex regulation of TNF biosynthesis via expression and phosphorylation of tristetraprolin, Biochem. Pharmacol 80 (12) (2010) 1915–1920. [PubMed: 20599781]

[67]. Lee HI, Rhim WK, Kang EY, Choi B, Kim JH, Han DK, A multilayer functionalized drug-eluting balloon for treatment of coronary artery disease, Pharmaceutics 13 (5) (2021).

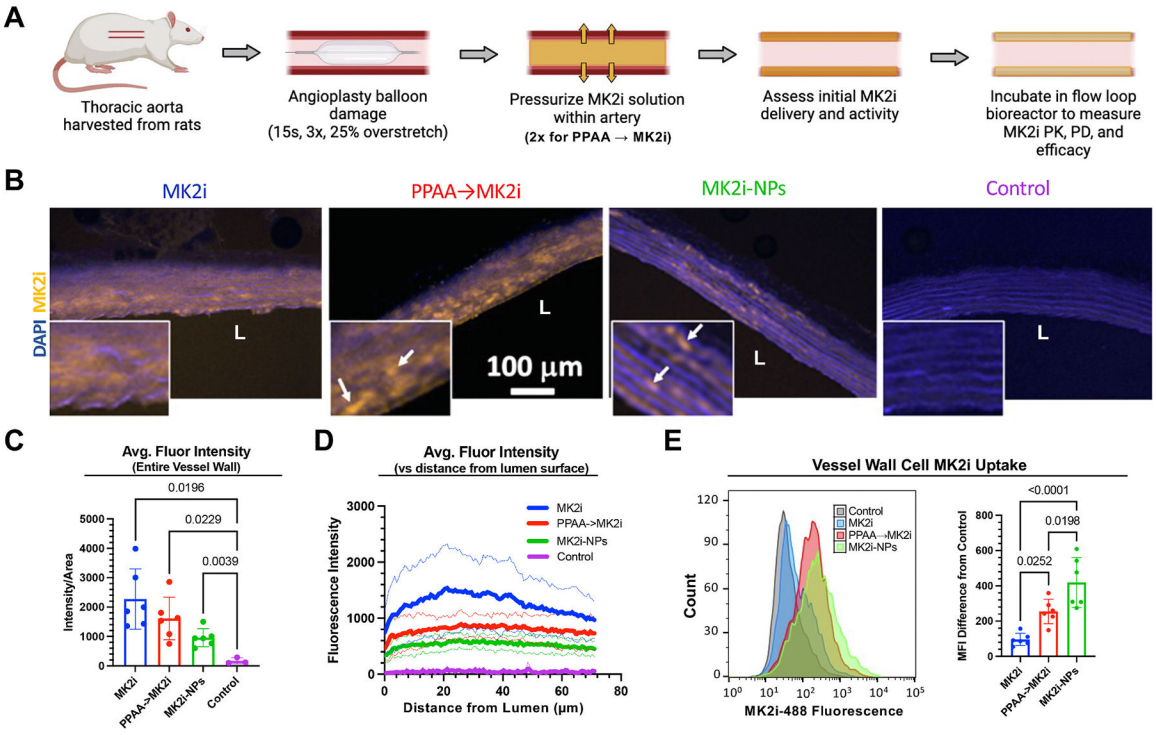

Fig. 1.

Convective delivery of MK2i to rat aortas *ex vivo*. (A) Treatment schematic for evaluating convective MK2i delivery in *ex vivo* rat aortas. (B) Confocal microscope images of rat aortas treated with free MK2i, PPAA→MK2i, or MK2i-NPs for 3 min. “L” marks the lumen side of each vessel. Arrows indicate cell-associated fluorescent MK2i. (C) Quantification of MK2i delivery to rat aortas. ROIs were drawn around the vessel wall and total intensity was normalized to the area of the vessel wall. N = 6. (D) Average MK2i fluorescence intensity profiles were quantified with respect to depth into the tissue from surface of the lumen. (E) Treated aortas were disaggregated, and uptake of fluorescent MK2i by cells within the tissue was quantified by flow cytometry. N = 6. Significance was determined using one-way ANOVA with Tukey’s post-hoc test.

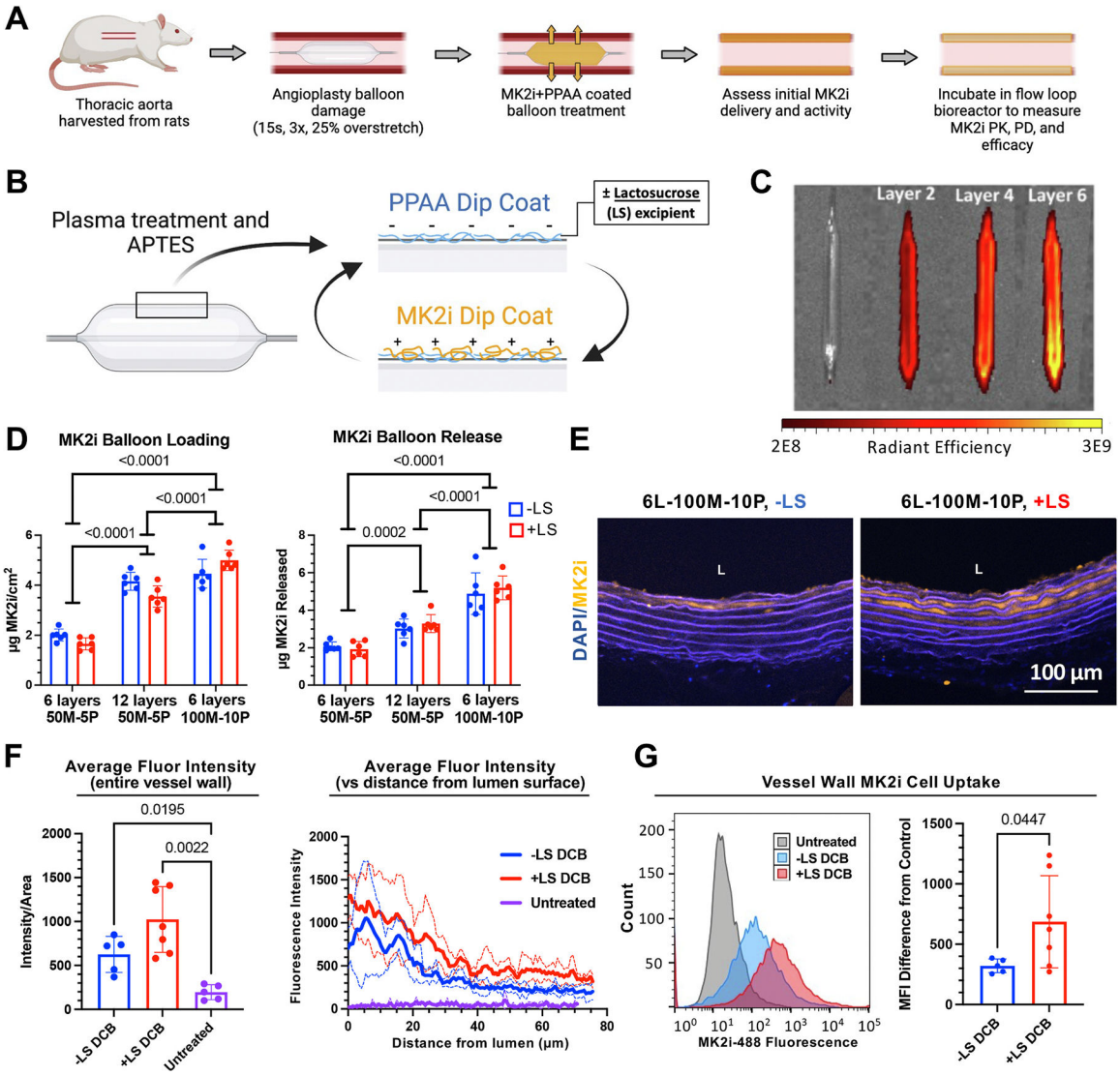

Fig. 2.

Angioplasty balloon coating and vessel delivery. (A) Schematic for experiments to test drug coated balloons *ex vivo*. (B) LbL coating scheme. (C) Visualization of fluorescent MK2i loading with addition of successive layers. (D) Comparison of MK2i drug loading and release for LbL conditions using varied numbers of layers and concentration of coating solutions. Significance determined using two-way ANOVA. N = 6. (E) Visualization of MK2i transfer from LBL coated balloons to *ex vivo* rat aorta immediately after balloon inflation for 6 layer, 100 µM MK2i, 10 µM PPAA (6 L-100M – 10P) balloons with or without LS. “L” marks the lumen side of each vessel. (F) Quantification of overall fluorescent MK2i delivery to vessel wall by 6 L-100M – 10P ± LS balloons and average intensity profile of fluorescent MK2i as a function of depth into the vessel wall. Significance was determined using on-way ANOVA with Tukey’s post-hoc test. N ≥ 5. (G) Treated aortas were disaggregated, and uptake of fluorescent MK2i by cells within the tissue was quantified by flow cytometry. Significance was determined using Welch’s *t*-test. N ≥ 5.

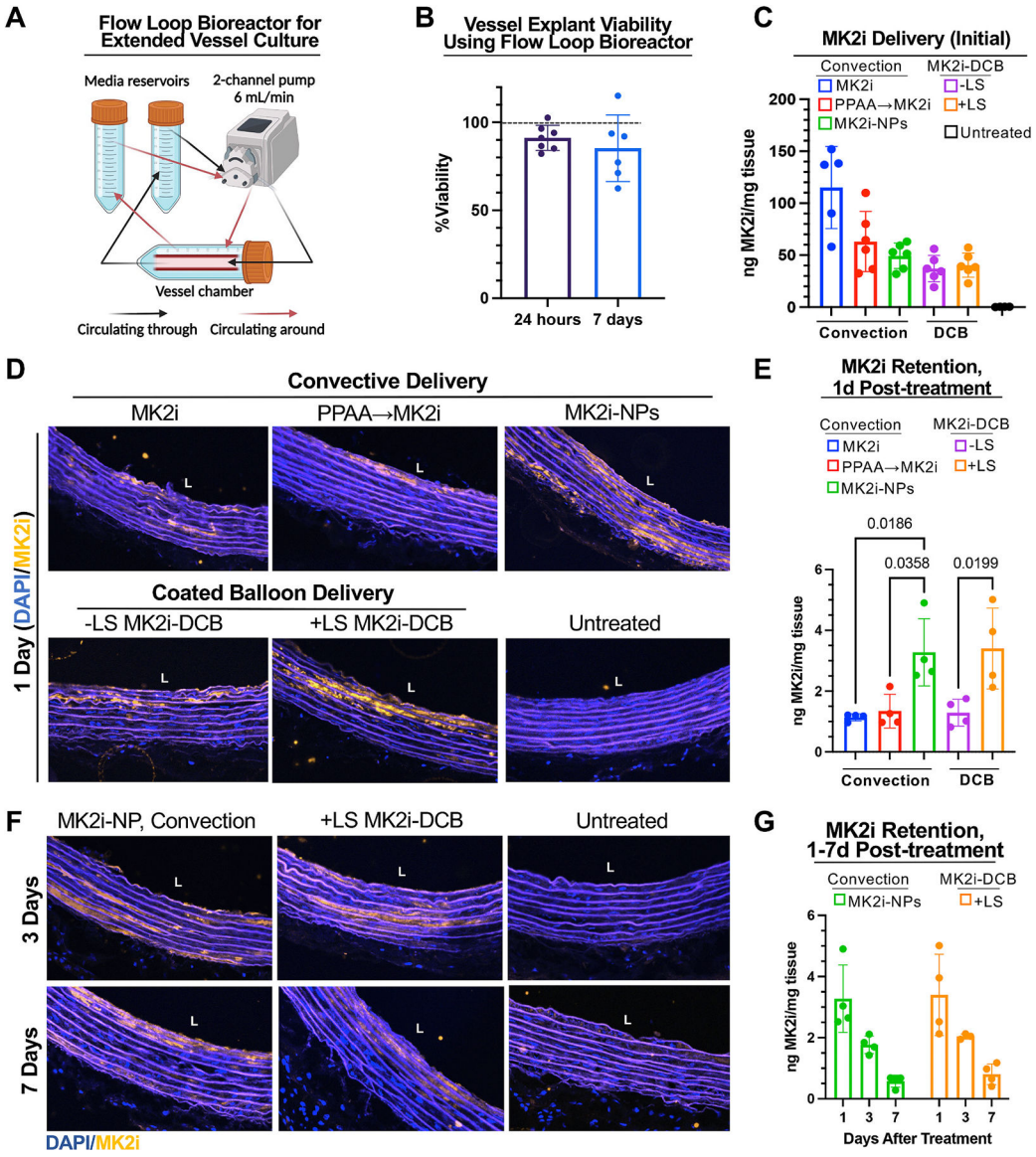

Fig. 3.

Pharmacokinetics of MK2i for different intravascular delivery approaches. (A) Schematic of flow loop bioreactor setup. (B) MTT assay measurement of viability on aortas housed in the flow loop bioreactor after 24 h or 7d compared to fresh aortas. (C) Quantification of MK2i in rat aortas immediately after *ex vivo* treatment. N ≥ 5. (D) Confocal microscope images of fluorescent MK2i treated rat aortas after 24 h in the flow loop bioreactor. “L” indicates the lumen side of each vessel. (E) Quantification of MK2i in the arterial tissue at 24 h after each treatment. Significance was determined with one-way ANOVA with Tukey’s post-hoc test. N = 4. (F) Confocal images of fluorescent MK2i retention after 3d and 7d incubation. (G) Quantification of MK2i in the aortas at 1-, 3-, and 7-days post-treatment for the two leading treatment strategies. N = 4.

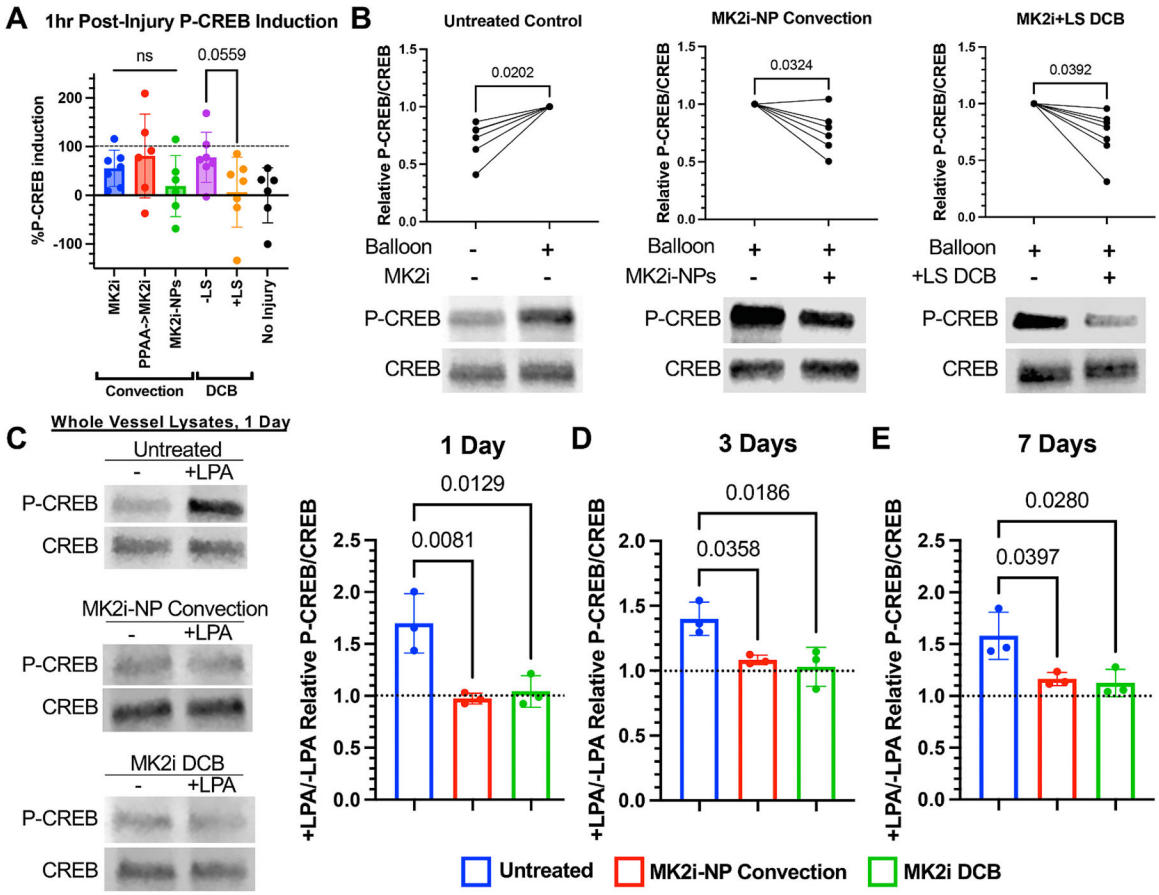

Fig. 4.

Pharmacodynamics of bioactivity of intravascular MK2i delivery techniques. (A) Convective MK2i-NPs and MK2i DCB administration blocks balloon damage induced CREB phosphorylation. The P-CREB induction was quantified with undamaged arteries serving as a baseline and balloon-damaged arteries without MK2i treatment representing 100 % P-CREB induction. (B) Pairwise comparisons were made between undamaged, untreated Control aortas and aortas treated with MK2i-NP convection or MK2i + LS coated balloons using a ratio paired *t*-test. N ≥ 6. Durability of MK2i activity was measured at (C) 24 h, (D) 3 days, and (E) 7 days by analyzing CREB phosphorylation. Half of each aorta was left unstimulated, and the other half was stimulated with LPA for 2 h to activate CREB. The relative amount of LPA-stimulated P-CREB was measured and compared across groups. N = 3. The p-values were determined using one-way ANOVA with Tukey's post-hoc test.

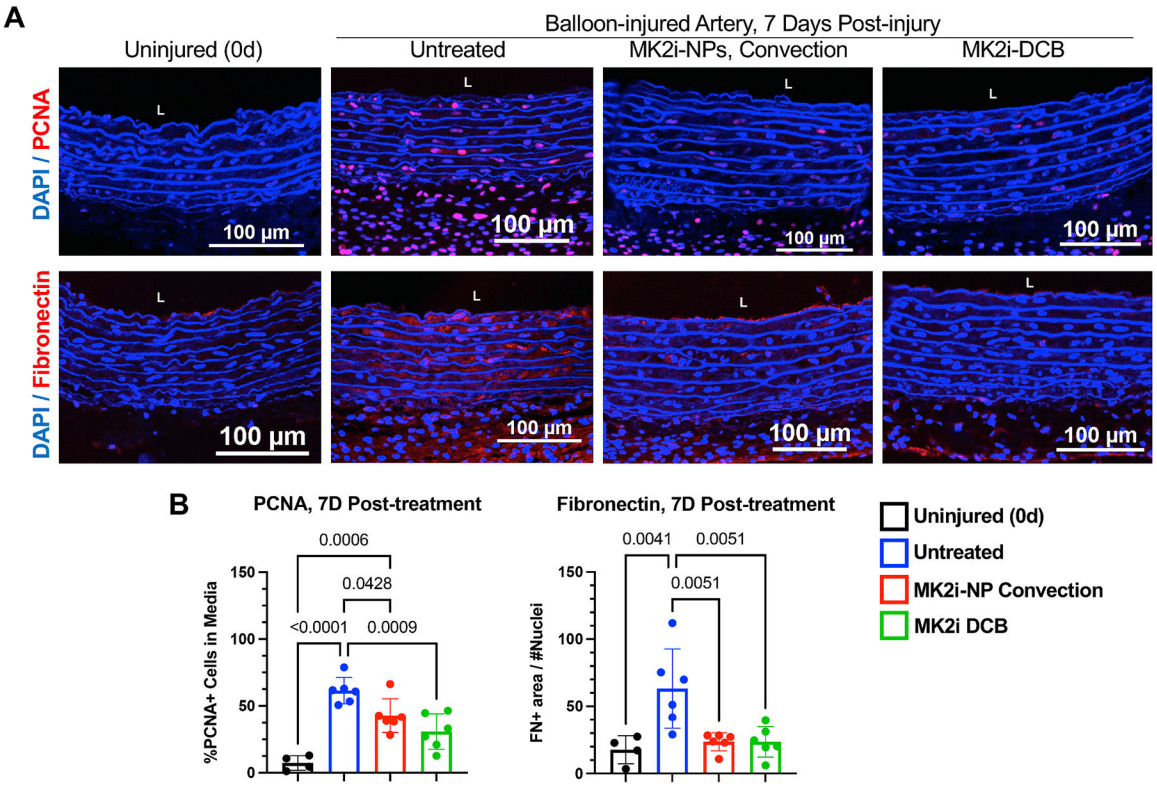

Fig. 5.

Intravascular MK2i treatments inhibit proliferation and ECM deposition, indicators of synthetic VSMC phenotype, in balloon-damaged *ex vivo* rat aortas maintained in dynamic culture. (A) Aortas cultured under flow in the bioreactor for 7d following balloon injury were stained with PCNA to quantify cellular proliferation. The percentage of PCNA positive cells in the media layer was calculated for each sample. (B) These same samples were immunohistochemically stained for fibronectin to assess ECM synthesis. “L” indicates the lumen side of each vessel. Fibronectin positive area was normalized to number of nuclei for the media layer of each sample. N = 6 for untreated, MK2i-NP, and MK2i DCB groups, N = 4 for uninjured control groups. The p-values were determined using one-way ANOVA with Tukey’s post hoc test.

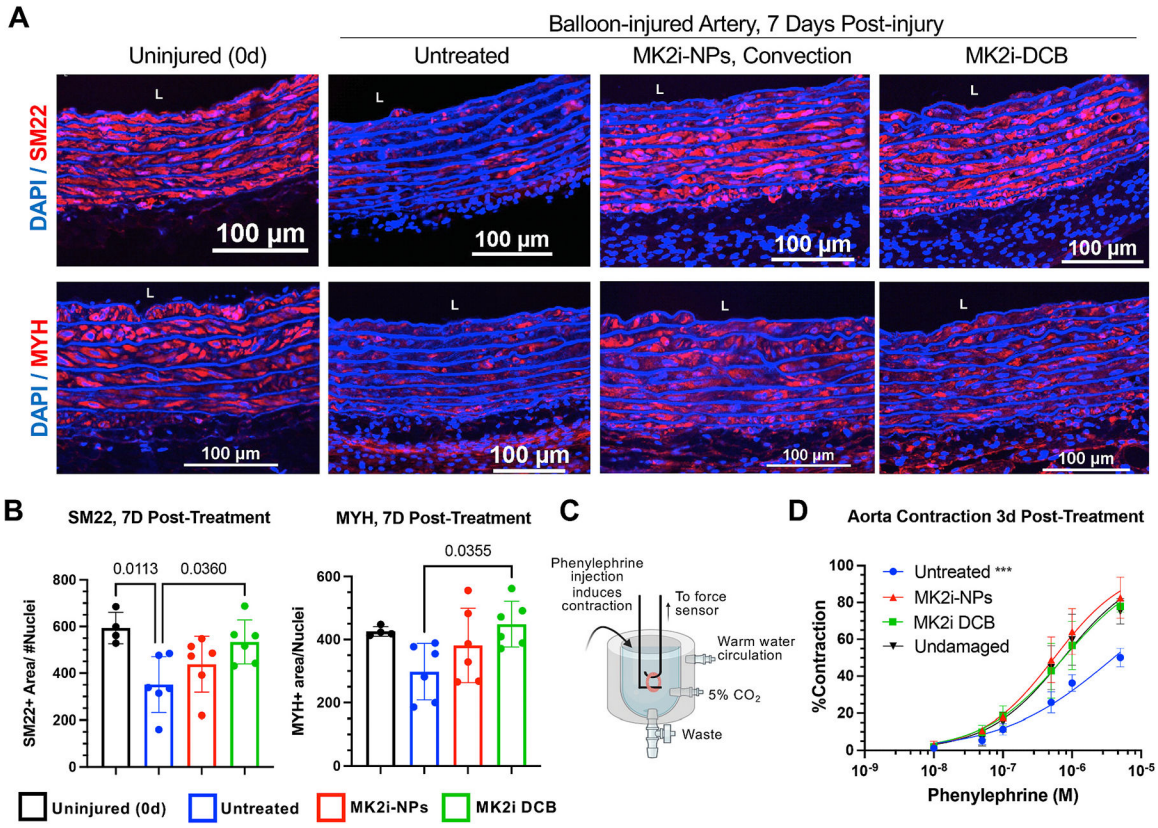

Fig. 6.

Intravascular MK2i treatments preserve VSMC contractile phenotype in balloon-damaged *ex vivo* rat aortas. (A) IHC for contractile protein SM22 and (B) MYH in aortas maintained under flow culture for 7d following balloon injury. “L” indicates the lumen side for each vessel. SM22/MYH positive area was normalized to number of nuclei for each sample. The p-values were determined using ANOVA and Tukey’s post hoc test. N = 6 for untreated, MK2i-NP, and MK2i DCB groups, and N = 4 for uninjured control groups. (C) Muscle bath contractility tests were performed after culture under flow for 3d post-injury. (D) Percent vessel contraction was measured in response to increasing concentrations of PE. Statistical significance was determined using an ANOVA and Tukey’s post hoc test on IC50 values determined from linear regression models of the PE vs contraction curves. N = 3. *** = $p < 0.005$ relative to Control, MK2i DCB, and MK2i NPs.

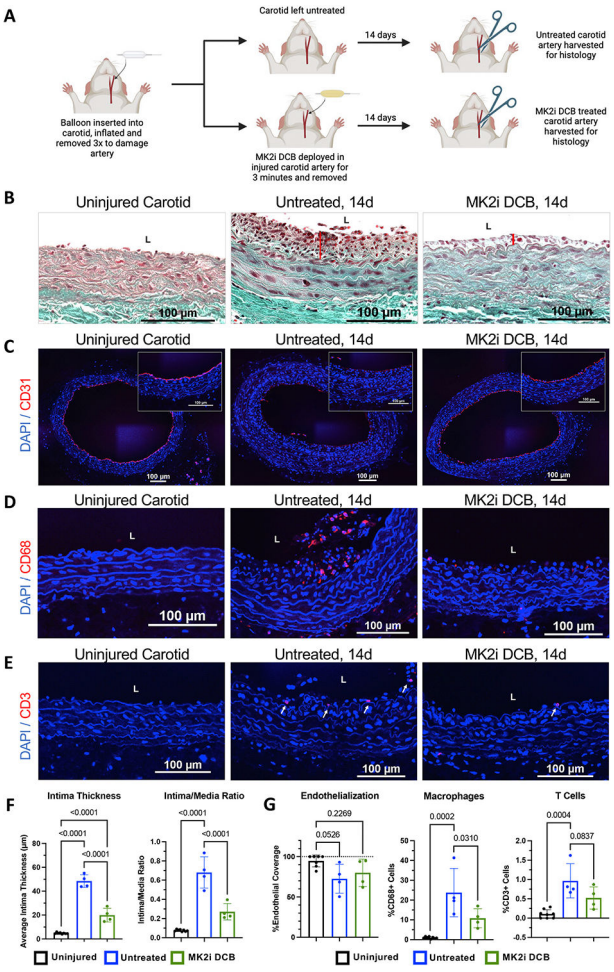

Fig. 7.

MK2i DCB treatment inhibits IH development and reduces immune cell infiltration, without impairing endothelialization. (A) Rat carotids were balloon damaged and either left untreated or treated with MK2i DCB. (B) Trichrome staining of rat carotid arteries 14d after injury, with red bars indicating neointimal development. “L” indicates lumen side for each vessel. (C) CD31 staining of carotid sections enables visualization of vessel endothelial coverage 14d after surgery. IHC was also used to visualize and quantify number of (D) $CD68^{+}$ macrophages and (E) $CD3^{+}$ T-cells in the tissue at the injury site. White arrows indicate $CD3^{+}$ cells. (F) Quantification of thickness of intima and intima to media ratio. (G) Quantification of IHC markers for endothelial cells and inflammation. T Cells were averaged across 3 different sections from each carotid. The p-values were determined with one-way ANOVA and Tukey’s post hoc test. N = 4 for untreated and MK2i DCB groups, N = 8 for uninjured groups.

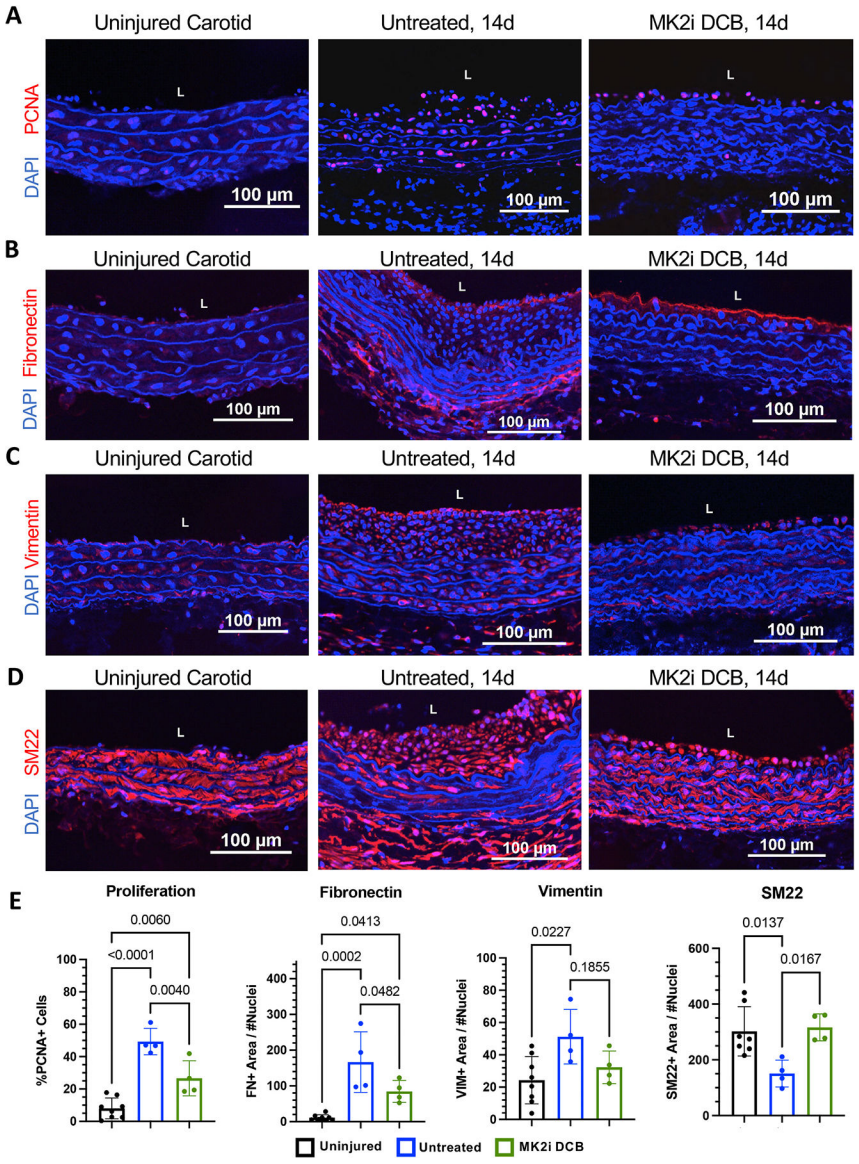

Fig. 8.

MK2i DCB treatment blocks VSMC contractile to synthetic phenotype switch *in vivo* at sites of carotid artery balloon injury. (A) PCNA was used as a marker of proliferating cells in carotid artery sections. Carotid artery injury site histological sections were also analyzed by IHC for (B) fibronectin and (C) vimentin, both markers of the synthetic VSMC phenotype, while IHC for (D) SM22 was used to assess the VSMC contractile phenotype. (E) IHC sections were quantified with ImageJ and normalized to number of nuclei for each marker. The p-values were determined with one-way ANOVA and Tukey's post hoc test. N = 4 for untreated and MK2i DCB groups, N = 8 for uninjured groups.